Fracture Mechanics of Concrete and Concrete Structures - Assessment, Durability, Monitoring and Retrofitting of Concrete Structures- B. H. Oh, et al. (eds)
ⓒ 2010 Korea Concrete Institute, Seoul, ISBN 978-89-5708-181-5

Experimental analysis and numerical simulation of permeability evolution in cracking concrete

H. Yang, Y. Liang, Y. Jia, and J.F. Shao
Laboratory of Mechanics of LILLE-University of Lille I, Cité Scientifique, 59655 Villeneuve d'Ascq, France

ABSTRACT: this paper contributes to the experimental anlysis and numerical simulation of permeability evolution on cracking concrete the studied concrete material, called CEM1, is the potential candidate for the underground storage for nuclear wastes. In the first part, an original experimental set-up is presented. The evolution of permeability was measured regularly during charge with pulse-test technique. The experimental result showed that the permeability of CEM1 had a significant variation due to the initiation and the development of volumetric contractance/diatancy and micro-cracking. The permeability increased tens of times when the crack happened. Based on the experimental investigation, the concrete material develops an important plastic deformation coupled with damage induced by micro-cracks. In view of this, a coupled elastopalstic damage model is formulated based on elastoplasticity and continuum damage mechanics. Finally, the performance of proposed model is evaluated by the simulation of experimental data.

1 GENERAL INSTRUCTIONS

The low permeability concrete can be used as the engineering background in many industrial and engineering applications. Especially in recent years, these types of material have been largely studied because they can be considered as potential engineering barrier for the underground storage of high level radioactive wastes. The studied concrete material, called CEM1, is the potential candidate for the underground storage for nuclear wastes requested by ANDRA (French National Agency for Nuclear Waste Management). A special adjuvant has been used in CEMI in order to reinforce its compressive resistance and elasticity module and also decrease its permeability. In this paper, the concrete is studied both experimentally and numerically for characterizing the coupling processes between its mechanical behavior and permeability. In the first part, an original experimental set-up is presented. The evolution of permeability was measured regularly during charge with pulse-test technique. More preciously, two confining pressures (5MPa, 10MPa) were exerted in the tests; the deviatoric stress was augmented until the failure of specimen. Meanwhile, the permeability was measured respectively before and after the peak of the deviatoric stress. The experimental result showed that the permeability of CEM1 had a significant variation due to the initiation and the development of volumetric compressibility, dilatancy, and micro-cracking. The permeability increased tens of times when the crack happened. Based on the experimental investigation, the concrete material develops an important plastic deformation coupled with damage induced by micro-cracks. In view of this, a coupled elastopalstic damage model is formulated based on elastoplasticity and continuum damage mechanics. In order to study the influence of water pore pres-sure, the effective stress conception is used. Finally, the performance of proposed model is evaluated by the simulation of experimental data.

2 STUDIED MATERIAL: CEMI

The studied material is the concrete of type CEM I. The concrete beam was prepared in the LML (Mechanic Laboratory in Lille). During 5 months of maturation, it was laying in a pool with the lime water in the temperature of 20C. The compositions of the concrete are presented in table 1.

Table1. Composition of the studied concrete (CEM I).

constituents	Nature	Dosage (kg/m^3)
Cement	CPA-CEM Ⅰ 52,5 PM ES CP2	400
Sand (0/4)	Limestone washed in 10 % of liqueur brandies 0/4 mm	858
Fine gravel(5/12,5)	Limestone washed 5/12,5	945
Adjuvating	Super plastifiant Glénium 27	10
Effective Water	Water	171
Characteristic of composition		
E/C		0,43
G/S		1.1

The concrete is poured into a coffering of beam with 2m of length and a section of 15cm*15cm. After 6 months of maturation in the lime water under temperature of 20°C, the samples were cored in the water, and then they were cut up and rectified to affect the wanted dimensions (cylinder having a diameter of 37mm and a height of 75mm).

2.1 *Experiment equipement*

The tests were performed with the aid of the system of autonomous and auto-compensable cell in LML. This system is composed of a conventional triaxial cell which is allowed for applying a confining pressure, of an upper room which makes it possible to exert an axial stress and of a circuit of interstitial fluid. The axial load is transmitted via the piston crossing the higher chapeau of the cell, the force on this one is applied by using a generator of pressure (here a Gilson pump). This system is also equipped with a compensating room making it possible to eliminate the force exerted by the confining pressure on the piston. The confining pressure is also applied by using a generator of pressure.

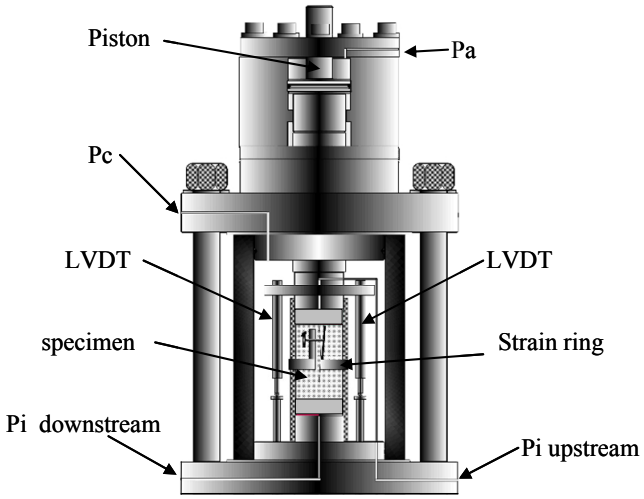

Figure 1. Illustration of the experimental device used.

In order to carry out the water Pulse-test, two buffer reservoirs are loaded on pressure to inject fluid on the lower side and upper side of the sample, by using two pumps. The signals of the rings of deformation and the LVDT, the data of the pumps, are recorded by an automatic central acquisition. A diagram of the experimental device is presented on figure 1.

2.2 *Testing procedure*

First, the samples are placed in a container under vacuum during 12 hours to accelerate the process of saturation. Then, it's the installation of the sample. To avoid the contact with the oil which transmits the confining pressure, the sample is sheathed in a Viton sleeve. Three rings for measuring the deformation radial are placed, respectively in 1/3, 1/2 and 2/3 of the height of the sample. Two LVDT sensors are settled at the two lateral sides parallel to measure axial displacement. Then, the sheathed sample is fixed to the plateau of the cell, a steel enclosure is placed all around, into which we inject the oil which is going to supply the confining pressure.

After the installation of the sample, the test process is summarized by the following steps:

- The confining pressure is loaded to the wished value, which is of 5MPa and 10MPa.
- The deviatoric stress is then increased to a value chosen; the values of the deviatoric stress for each confining pressure are indicated in Table 2.
- In this state of stress chosen, the fluid of type "pulse- test" in transitory regime is injected. For that purpose, both pressures of injection (in the lower and upper surfaces of the sample) are increased and maintained in 2MPa during 20 minutes using of two buffer reservoirs.
- Then the pressure of injection of the lower surface of the sample is increased to 2.5MPa. Lastly, we stop the injection of fluid and record the variations of the two pressures during one period of approximately 30 minutes. A general diagram for the route of loading is shown on Figure 2.
- The deviatoric stress is loaded up to a higher level.

Table2. Values of the deviatoric stress chosen for puls-test.

Confining pressure σ_3 (MPa)	Deviatory stress $\sigma_1 - \sigma_3$ (MPa)		
5	75.9	97.9	64
10	53.7	110	79.8

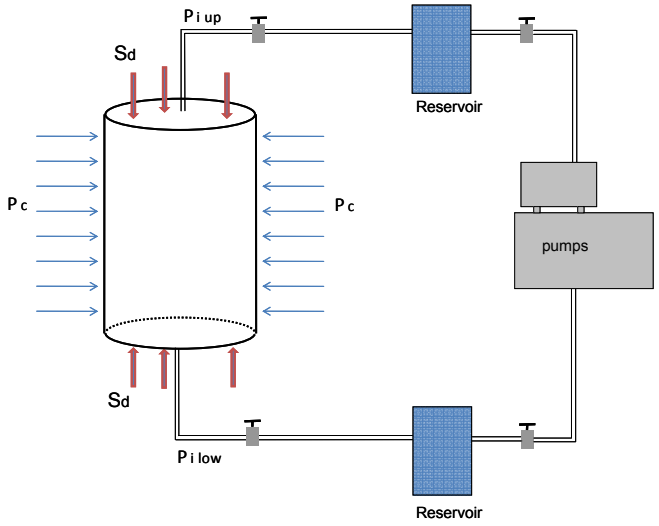

Figure 2. General diagram for the route of loading.

3 EXPERIEMENTAL RESULTS

In figure 3, the results representative represent of the test with a confining pressure of 5MPa. It shows the typical characteristics of a concrete in a triaxial compression test. The mechanical answers nonlinear are characterized by a coupling of the plastic deformation with the damage induced by microscopic cracks. The macroscopic rupture is marked by a peak of resistance followed by a phase of radoucissement. The behavior radoucissant in a concrete is generally related to the damage induced by the propagation of microscopic cracks.

With regard to the variations of the two fluid pressures on the sample, generally, those decrease gradually following the diffusion of fluid towards the interior of the sample. It's presented clearly that the kinetics of reduction depends on the level of the deviatoric stress; the pressures decrease more quickly when the deviatoric stress is higher. This shows that the permeability becomes larger with the increase in the deviatoric stress. Thus, there is a coupling between the permeability and the level of damage which increases with the deviatoric stress. It is interesting to note that the voluminal dilatancy is not so important during loading deviatoric. It seems that the damage by micro-fissuring affects primarily the permeability, without inducing significant voluminal dilatancy

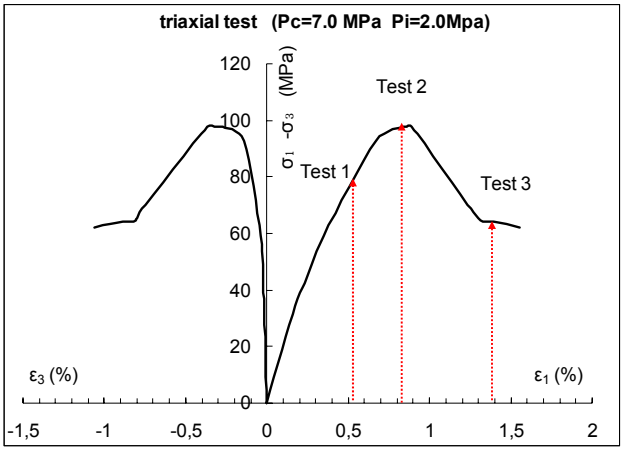

(a)

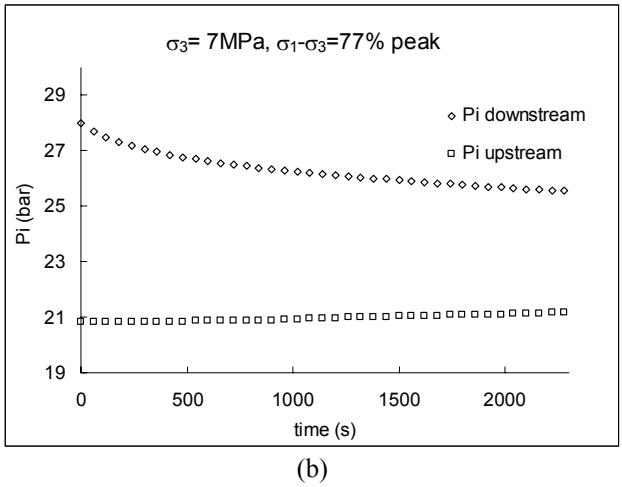

(b)

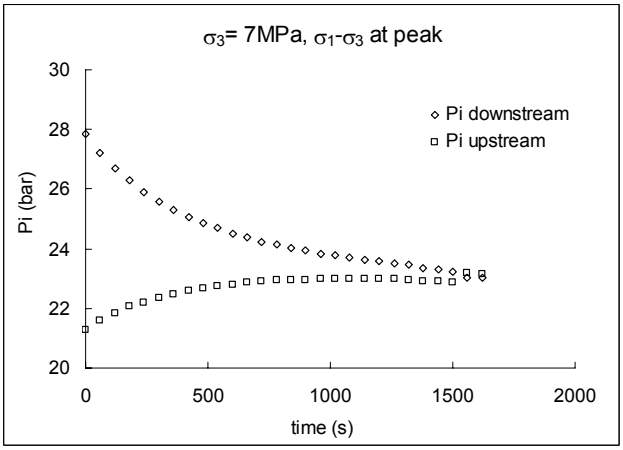

(c)

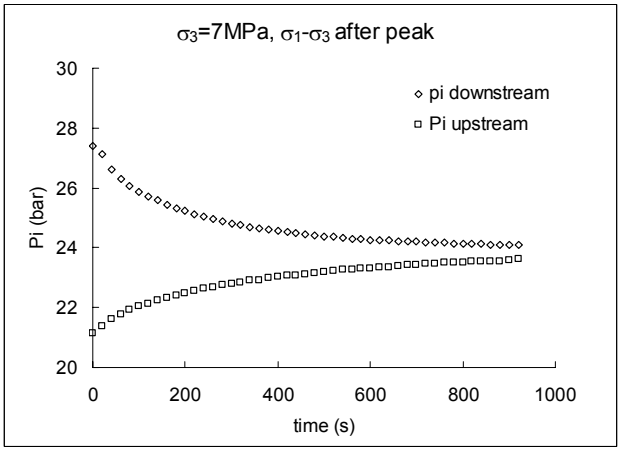

(d)

Figure 3. Results obtained of the test with 5MPa confining pressure; (a) curves of the stress and strain, (b) (c) (d) variations of the pressures according to time.

4 ELASOPLASTIC DAMAGE CONSTITUTIVE MODEL

In this section, a brief synthesis of the constitutive model for CEMI is presented. An isotropic damage is assumed and represented by the scalar variable ω. In order to take into account the effects of liquid and gas pressures, an equivalent pore pressure π is used and then the elastic constitutive relative are expressed as following:

$$\sigma_{ij} = \left(k_b(\omega) - \frac{2}{3}\mu(\omega) \right) tr(\varepsilon^e)\delta_{ij} + 2\mu(\omega)\varepsilon^e_{ij} - b(\omega)\pi\delta_{ij} \tag{1}$$

$k_b(\omega)$, $\mu(\omega)$ and $b(\omega)$ are respectively the effective drained bulk and shear modulus and Biot's coefficient of damaged material.

4.1 *Plastic modeling*

As mentioned in the previous section, the effective stress tensor is also used for plastic modeling of partially saturated materials in order to take into account the effects of pore pressure.

$$\sigma_{ij}^{pl} = \sigma_{ij} + \beta(\sigma, S_l)\pi\delta_{ij} \tag{2}$$

As results, the yield function and the plastic potential are proposed with the plastic effective stress:

The yield function

$$f_p(\sigma_{ij}, \eta) = \tilde{q} - g(\tilde{\theta})\eta(C_s + \frac{\tilde{p}}{P_a}) = 0 \tag{3}$$

$\tilde{p}, \tilde{q}, \tilde{\theta}$ are, respectively, the mean stress (compressive mean stress is taken as positive), deviatoric stress and Lode's angle. The parameter Cs represents the hydrostatic tensile strength corresponding to the intersection of the failure surface with the mean stress axis (see Fig. 1). The function $g(\tilde{\theta})$ allows accounting for the dependency of yield function on the Lode angle in the deviatoric plane.

The plastic hardening is characterized by the variation of the coefficient η, as a function of the generalized plastic shear strain noted by γ_p. The variable η increases with the plastic strain γ_p, but decreases with the damage variable ω. Based on the experimental data from triaxial compression tests, the following function is proposed:

$$\eta(\gamma_p, \omega) = (1-\omega)\left[\eta_0 + (\eta_m - \eta_0)\frac{\gamma_p}{b_1 + \gamma_p}\right] \tag{4}$$

The plastic potential

$$Q = \tilde{q} + \mu_c(1-\omega)g(\theta)(\tilde{p} + P_a C_s)\ln\left[\frac{\tilde{p} + P_a C_s}{\bar{p}}\right] = 0 \tag{5}$$

The coefficient $\bar{p}$ corresponds to the intersection point between the plastic potential surface and the axis $\tilde{p} + P_a C_s$. The coefficient $\mu_c(1 - \omega)$ represents the ratio $\tilde{q} / g(\theta)(\tilde{p} + P_a C_s)$ at the points with $\partial Q / \partial \tilde{p} = 0$; i.e. the transition boundary between volumetric compressibility and dilatancy.

4.2 *Damage modeling*

Based on the previous works performed by Mazars (1984), it is assumed that the damage is divieded into two sections: ω_c damage generated by the compression and ω_t damage generated by the traction:

$$\omega = (1-\alpha_t)\omega_c + \alpha_t\omega_t \tag{6}$$

They are respectively defined by the following function:

$$\omega_c = 1 - \frac{1}{\exp\left(B_t, Y_t^{\omega}\right)} \quad , \quad Y_t^{\omega} = \varepsilon_{eq} \tag{7}$$

$$\omega_c = 1 - \frac{1}{\exp\left(B_c, Y_c^{\omega}\right)} \quad , \quad Y_c^{\omega} = \left\langle \gamma_p \right\rangle \tag{8}$$

The coefficient α_t depends on the stress state.

$$\varepsilon_{eq} = \sqrt{\sum_{i=1}^{3} \left\langle \varepsilon_i \right\rangle^2} \tag{9}$$

The parameters (B_t and B_c) control the kinetics of tensile and compressive damage evolution. ε_i (i =1, 2, 3) represents three principal strains.

4.3 *Permeability law*

The relationship between the permeability variation and damage induced in material can be formulated theoretically based on homogenization technique (Dormieux & Lemarchand, 2001) These approaches provide a justification of the relationship for the coupling between the permeability and the crack growth. However, the damage is irreversible; it can only represents the density of cracks, no matter the cracks are opening or re-closing. As a simple example, the fissure created by traction test, it has the same damage value when the fissure has been created and re-closed, but the permeability in the fissured state is much larger than the re-closed state. Considering the most essential element which generates the permeability is the width of the cracks, we use the concept of equivalent strain ε_{eq} which characterize the dilatability of material during the loading to characterize the total width of cracks.

$$K = K_0\left[1 + m\left(1 - \frac{1}{\exp(N \cdot \varepsilon_{eq})}\right)^2\right] \tag{10}$$

The parameter N controls the kinetics of permeability evolution; the parameter m controls the amplitude maximum of permeability; and the parameter ε_{eq} represents the equivalent strain. K_0 is the material's initial permeability 3E-21m^2.

5 NUMERICAL SIMULATIONS

The laboratory tests preformed in our laboratory are simulated in this part. The experimental data from the triaxial tests have been used for the determination of the model's parameters. Using these parameters, numerical simulations of laboratory tests have been performed and some examples are given here.

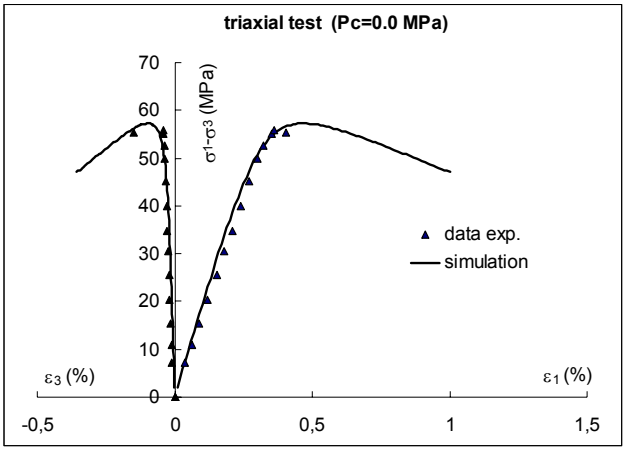

(a)

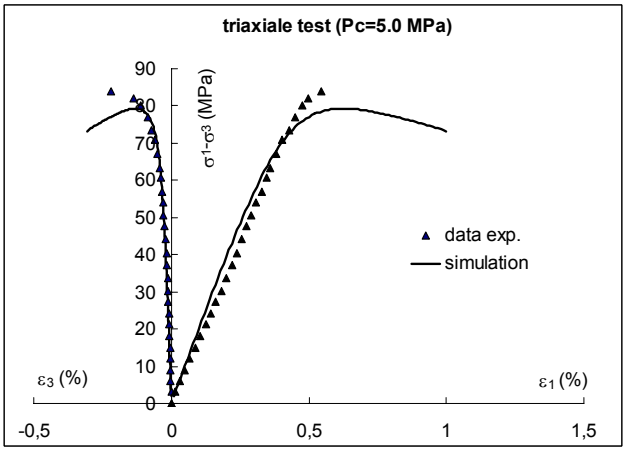

(b)

Figure 4. The simulation results of tri-axial test: (a) 0MPa confining pressure, (b) 5MPa confining pressure.

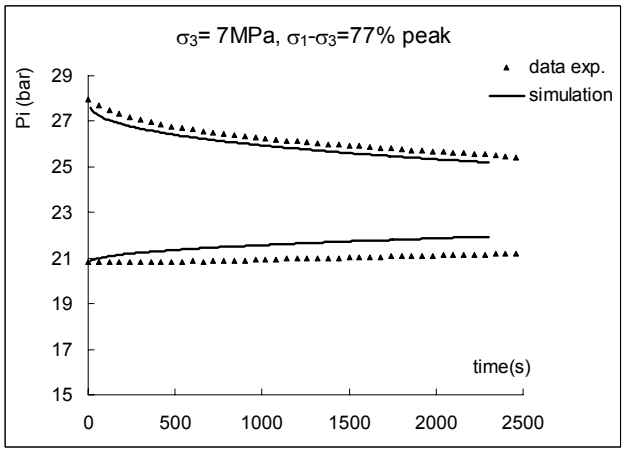

(a)

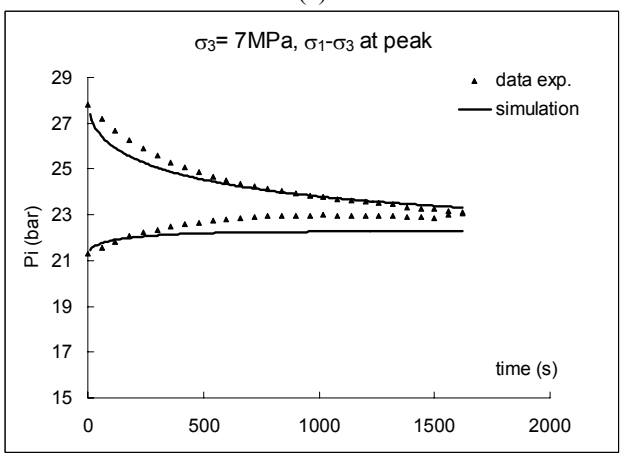

(b)

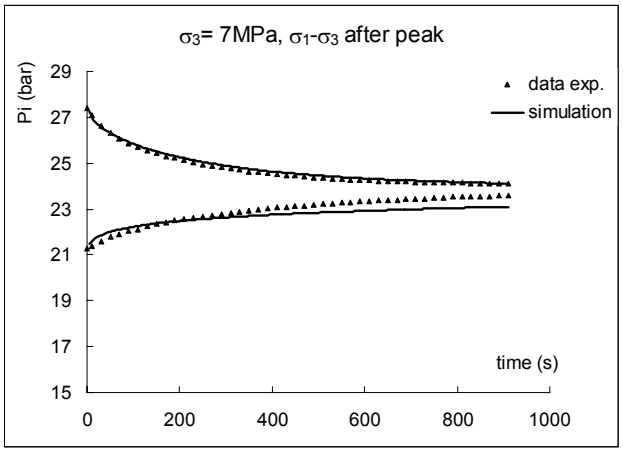

(c)

Figure 5. The simulation results of the pulse test at 7MPa confining pressure.

In the test, the input and output pressure is respectively measured on the bottom and top of the simple Figures 3 shows the pressure evolution for different strain state under 7MPa confining pressures. Note that these tests have been used for the determination of model's parameters. Therefore, these simulations represent a direct verification of the consistency of the formulation and the determination procedure of parameters. There is a good agreement between the simulations and experimental data. The material's permeability varied from 3E-21m^2(initial value) to 5E-19m^2 (value after peak).

6 CONCLUSIONS

A new experimental analysis and an elastoplastic damage model are proposed for the permeability law of cement material. The simulations of laboratory tests have shown a good agreement with experimental data. The mathematical formulation of the model is simple and can be easily implemented in a finite element code. The proposed model is able to describe the main features of hydromechanical behaviours of the argillite formation, such as plastic strain, material damage by microcracks, pressure sensitivity, and transition from volumetric compressibility to dilatancy. The application examples are presented on the poromechanical modelling of pulse-test with a variation of stress state. It has been noted that time-dependent plastic deformation and damage are induced by mechanical loading. The evolution of pore pressure is mainly controlled by the variation of the intrinsic permeability. In conclusion, the proposed model is capable of reproducing the important coupling between hydraulic flow and mechanical behaviour of this concrete material. In the near future, it will be used to simulate the coupled hydro-mechanical behaviour of underground waste disposal facilities during the exploration and post-closure periods.

REFERENCES

Dormieux L, Lemarchand E. 2001. Homogenization approach of advection and diffusion in cracked porous materials. Journal of Engineering Mechanics (ASCE) 2001; 127:1267–1274.

J.F. Shao, Y. Jia, D. Kondo and A.S. Chiareli, 2006.A coupled elastoplastic damage model for semi-brittle material and extension to unsaturated conditions. 218–232.

Mazars. J.1984. Application de la mécanique de l'endommagement non linéaire et à la rupture du béton de structure. Doctoral Thesis, vol. 6. University of Paris;. [in French].